JCTC Journal of Chemical Theory and Computation

Static and Dynamical Properties of Liquid Water from First Principles by a Novel Car−Parrinello-like Approach

Thomas D. Kühne,*,† Matthias Krack,†,‡ and Michele Parrinello†

Computational Science, Department of Chemistry and Applied Biosciences, ETH Zurich, USI Campus, Via Giuseppe Buffi 13, CH-6900 Lugano, Switzerland

Received October 3, 2008

Abstract: Using the recently developed Car−Parrinello-like approach to Born−Oppenheimer molecular dynamics (Kühne, T. D.; et al. *Phys. Rev. Lett.* 2007, *98*, 066401.), we assess the accuracy of ab initio molecular dynamics at the semilocal density functional level of theory to describe structural and dynamic properties of liquid water at ambient conditions. We have performed a series of large-scale simulations using a number of parameter-free exchange and correlation functionals, to minimize and investigate the influence of finite size effects as well as statistical errors. We find that finite size effects in structural properties are rather small and, given an extensive sampling, reproducible. On the other hand, the influence of finite size effects on dynamical properties are much larger than generally appreciated. So much so that the infinite size limit is practically out of reach. However, using a finite size scaling procedure, thanks to the greater effectiveness of our new method we can estimate both the thermodynamic value of the diffusion coefficient and the shear viscosity. The hydrogen bond network structure and its kinetics are consistent with the conventional view of tetrahedrally coordinated water.

1. Introduction

Since the first applications of molecular dynamics (MD) to realistic systems,[1] liquid water has been one of the most studied systems, as it is arguably the most important liquid for its role in biology, chemistry, and geophysics. This widespread interest has also sparked many controversies, the most recent being the suggestion that the average coordination of water is 2 rather than 4 as the tetrahedral coordination of ice and the nature of the hydrogen bond (HB) would suggest.[2] A detailed understanding of liquid water is therefore essential and at the same time demanding due to its complex behavior and unusual properties.[3] However, simulating water is rather challenging due to the presence of a number of difficulties in modeling the various physical effects that conspire to make water unique, such as sizable quantum corrections, large permanent dipoles and strong polarizability effects, and the cooperativity of the HB network.

Much effort has gone into developing empirical potentials for water capable of describing all of these effects and much progress has been reported.[4−10] However, often the transferability of these potentials to regions of the phase diagram or systems different from that in which they have been fitted is restricted. Furthermore, they are not able to simulate with sufficient predictive power chemical processes that take place in water solutions.

A first-principles based approach, like density functional theory (DFT)[11] based ab initio molecular dynamics (AIMD), where the forces are evaluated on the fly from accurate electronic structure calculations, is very attractive since many of these limitations can in principle be removed. However, also the ab initio approach is not without problems: the relevant energy scale is very small and an error of 0.3 kcal/mol might cause the simulated water either to freeze or to evaporate. This poses very stringent accuracy constraints. Furthermore, the computational cost associated with AIMD has forced in the past numerical approximations to extend the attainable size and length scales of the simulation, and a significant dependence on numerical details has been reported.[12−19]

* Corresponding author. E-mail: tkuehne@phys.chem.ethz.ch.
† ETH Zurich.
‡ Current address: Paul Scherrer Institute, CH-5232 Villigen PSI, Switzerland.

10.1021/ct800417q CCC: $40.75
Published on Web 01/09/2009

In view of great potential impact and widespread interest, it is of great value to assess its intrinsic properties as distinct from those that descend from numerical approximations, finite size effects, and insufficient sampling. This is now made possible by a new simulation method[20] which is highly accurate and at the same time at least 1 order of magnitude more efficient than previous ones. In this work, we focus on the Perdew−Burke−Ernzerhof (PBE) approximation to the exact exchange and correlation (XC) functional, whose parameters have been determined from first principles.[21] We find that ordinary PBE water at 300 K is somewhat overstructured and less fluid than real water, with a shear viscosity (here calculated for the first time) which is within a factor of 3 of the experimental one. Given the fact that here nuclear quantum effects are not included, one can conclude that PBE does provide a qualitative realistic model for water−water interactions.

The long runs (∼250 ps) on relatively large systems (128 molecules) allow for the first time a number of dynamical properties to be evaluated with accuracy. We have already mentioned shear viscosity, and to this we can add the self-diffusion coefficient, which exhibits stronger than expected finite size effects, but whose asymptotic value for an infinite large system is now evaluated. We also calculate the single-particle velocity−velocity autocorrelation function and the corresponding power spectrum. In view of the current controversy, we have also examined the HB network and its dynamics. But eventually PBE water is consistent with the conventional wisdom, and this conclusion is not altered if other XC functionals are used.

However, before discussing our results we briefly summarize the principles that are at the bases of our method and is the key to our successful investigation and which has already found a number of practical applications.[22,23]

2. Second Generation Car−Parrinello MD

Contrary to the direct Born−Oppenheimer MD (BOMD),[24] in which during the dynamics the energy functional is fully optimized subject to the orthonormality constraint $\langle\psi_i(r)|\psi_j(r)\rangle = \delta_{ij}$, in the Car−Parrinello MD (CPMD)[25] approach this is circumvented by designing a suitable electron-ion dynamics in which, under appropriate conditions, the electrons follow adiabatically the ions very close to the instantaneous electronic ground state. An important role in this approach is played by μ, the fictitious electronic mass, which has to be chosen small enough to ensure this adiabatic decoupling.[26] As a consequence, the maximal permissible integration time step Δt has to be considerably smaller than in BOMD.[27] In our novel approach the original fictitious Newtonian dynamics of the electronic degrees of freedom is replaced by an another, very close to the Born−Oppenheimer (BO) dynamics, which does not require the introduction of any artificial mass. At variance with CPMD, where the electronic dynamics is defined by the introduction of a Lagrangian, the coupled electron−ion dynamics is directly specified. These are based on the always stable predictor−corrector method[28,29] of Kolafa, though other choices are equally possible.[30,31]

Let us represent the set of electronic wave functions in the form of a coefficient matrix **C** that has the dimension of the basis set size times the number of occupied states, which is assumed to be nonorthogonal. Thus, the overlap matrix **S** is different from unity. In terms of **C** and **S** we can now define the contracovariant density matrix **PS**, where $\mathbf{P} = \mathbf{C}\mathbf{C}^T$ is the one-particle density kernel. One expects that the dynamics of **PS** to be much smoother than that of the more widely varying wave functions even in the case of metals, where many states crowd the Fermi level. This consideration therefore suggests to propagate **PS**, rather than the wave functions as in CPMD.

2.1. Coupled Electron−Ion Dynamics. Adapting Kolafa's method to this particular case, we write the predicted wave function at time t_n in terms of K previous **PS** matrices as

$$\mathbf{C}^p(t_n) \cong \sum_{m=1}^{K} (-1)^{m+1} m \frac{\binom{2K}{K-m}}{\binom{2K-2}{K-1}} \mathbf{P}(t_{n-m})\mathbf{S}(t_{n-m})\mathbf{C}(t_{n-1}) \tag{1}$$

The corresponding corrector involves the evaluation of only one preconditioned electronic gradient MIN[**C**(t)] using the orbital transformation (OT) method of VandeVondele and Hutter.[32] This leads to the corrected **C**(t_n):

$$\mathbf{C}(t_n) = \omega \mathrm{MIN}[\mathbf{C}^p(t_n)] + (1-\omega)\mathbf{C}^p(t_n) \tag{2}$$

$$\text{with} \quad \omega = \frac{K}{2K-1} \text{ where } K \geq 2$$

Such a predictor−corrector scheme leads to an electron dynamics which is accurate and time reversible up to $\mathcal{O}(\Delta t^{2K-2})$, where Δt is the integration time step. The efficiency of this approach is such that the ground state is very closely approached within just one such step. We thus totally avoid the self-consistency cycle and any expensive diagonalization, while remaining very close to the BO surface and allow for Δt to be as large as in standard MD.

Nevertheless, a small dissipative energy drift is introduced that needs to be corrected. To this effect, in ref 18 we have shown, that an excellent model for the ionic forces thus calculated is $\mathbf{F}_\mathrm{I}^\mathrm{PC} = \mathbf{F}_\mathrm{I}^\mathrm{BO} - \gamma_\mathrm{D} M_\mathrm{I} \dot{\mathbf{R}}_\mathrm{I}$, where $\mathbf{F}_\mathrm{I}^\mathrm{BO}$ are the correct BO forces, γ_D a friction coefficient, M_I the ionic masses, and R_I the ionic coordinates. The presence of damping suggests a canonical sampling of the Boltzmann distribution based on a Langevin approach, rather than a microcanonical one. We therefore introduce a properly modified Langevin equation,[33] in which for convenience an additional friction coefficient γ_L is present. These damping terms are compensated by an additive white noise $\Xi_I(t)$, which is related to $\gamma = \gamma_\mathrm{D} + \gamma_\mathrm{L}$ by the fluctuation−dissipation theorem $\langle \Xi_\mathrm{I}(0)\Xi_\mathrm{I}(t)\rangle = 2\gamma M_\mathrm{I} k_\mathrm{B} T \delta(t)$, thus leading to an exact sampling.

In order to determine the unknown value of γ_D, we perform a preliminary run in which we vary γ_D on the fly using a Berendsen-like algorithm[34] until the equipartition theorem is satisfied. This can be somewhat laborious, but once γ_D is fixed, very long and accurate simulation runs can be performed at a much reduced computational cost, thus unifying the best of conventional BOMD and CPMD, since

one uses large time steps, while at the same time preserving the Car−Parrinello efficiency.

3. Computational Details

In the largest simulated system, we take a periodic cubic box of length $L = 15.6627$ Å consisting of 128 light water molecules that corresponds to a density that differs by only 0.3% from the experimental value. All simulations are performed at 300 K; the Langevin dynamics is integrated using the algorithm of Ricci and Ciccotti.[34] The discretized integration time step $\Delta t = 0.5$ fs, while $\gamma_D = 8.65 \times 10^{-5}$ fs^{-1} and $\gamma_L = 1.35 \times 10^{-5}$ fs^{-1}. The simultaneous propagation of the electronic degrees of freedom proceeds with $K = 7$, which yields a time reversibility of $\mathcal{O}(\Delta t^{12})$. At each MD step the corrector is applied only once, which implies just one preconditioned gradient calculation. The deviation from the BO surface, as measured by the preconditioned mean gradient deviation is 10^{-5} au, which is only slightly larger than typical values used in fully converged BOMD simulations.

Since we are dealing with a disordered system at finite temperature that also exhibits a large band gap, the Brillouin zone is sampled at the Γ-point only. Furthermore, separable and norm-conserving pseudopotentials are used to describe the interactions between the valence electrons and the ionic cores.[35−37]

Long and well-equilibrated trajectories are necessary in order to obtain an accurate sampling. This requirement is made even more stringent by the strong dependence of the translational self-diffusion coefficient on temperature and, in the case of PBE water, on the expected low diffusivity at room temperature.[16,38] Unless otherwise stated, we use the PBE generalized gradient approximation to the XC energy. In each run we equilibrate carefully the system for 25 ps and accumulate statistics in the successive 250 ps. Finite size effects are studied by comparing the results of the largest system with equally long runs on 64 and 32 water molecules. For the purpose of addressing the accuracy of our simulations, we have carried out two shorter, 25 ps long, reference calculations with 128 molecules, using fully self-consistent BO forces and either Newtonian or Langevin dynamics. Otherwise, the settings for both runs were identical and started from the same well-equilibrated configuration. We also investigated the influence of the XC functional in a series of additional runs using a variety of different semilocal XC functionals, either parameter-free,[39,40] or empirically parametrized.[41−43] In each of these reference runs, statistics were accumulated for at least 30 ps after an equilibration of 20 ps, totaling more than 1 ns of AIMD simulations.

All simulations were performed using the mixed Gaussian and plane wave[44] code CP2K/Quickstep.[45] In this approach, the Kohn−Sham (KS) orbitals are expanded in Gaussians, while for the electron density a plane wave basis is used. Exploiting the efficiency of transformation methods to alternate between one representation and the other, together with advanced multigrid, sparse matrix and screening techniques, an efficient linear-scaling evaluation of the KS matrix is obtained. Efforts towards a full linear scaling algorithm are underway.[47] Here the orbitals are represented by an accurate triple-ζ basis set with two set of polarization functions (TZV2P),[48] while a density cutoff of 320 Ry is used for the charge density. The use of a position-dependent basis set inevitably entails a basis set superposition error (BSSE). In our case the BSSE, as estimated by the average error in the binding energy of a single water molecule within the bulk against counterpoise corrected reference calculations at the complete basis set limit, corresponds to an approximately constant energy shift of 0.3 kcal/mol. Since the associated standard deviation is well below 0.01 kcal/mol, the nuclear forces as well as the chemical relevant energy differences are basically unaffected.

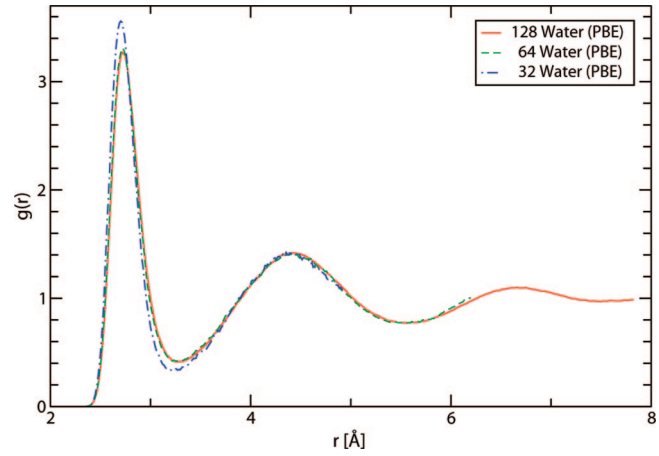

Figure 1. Comparison of the oxygen−oxygen PCF's, obtained from AIMD simulations, using 32, 64, or 128 water molecules.

4. Results and Discussion

4.1. Structural Properties. In Figure 1 the oxygen−oxygen pair-correlation function (PCF) $g_{OO}(r)$ evaluated on systems with different numbers of molecules are compared to assess the convergence with respect to system size. We find that, using 32 water molecules, errors due to finite size effects are not entirely negligible. However, already in the 64-molecule system the $g_{OO}(r)$ coincides, within statistical uncertainty, with that of the larger 128-molecule calculation, providing results that are converged with respect to system size.

In Figure 2 the partial pair correlation functions are compared to recent X-ray scattering[51] and neutron diffraction[48] data, but also to BOMD reference calculations in order to assess the accuracy of our novel approach. The agreement with the reference BOMD calculation is excellent, and the results are consistent with those of others.[12,14,16,38] Comparison with experiments reveals a general overstructuring and an oxygen−hydrogen PCF, whose relative heights of the first two intermolecular peaks are reversed. However, the inclusion of nuclear quantum effects is expected to further improves the agreement with experiments,[52] though probably less than earlier calculations suggested.[53] In the literature, PCF's in slightly better agreement with experiment have been reported; however, such calculations have been performed either at higher temperatures[12,13,15,16] or using different XC functionals.[17−19]

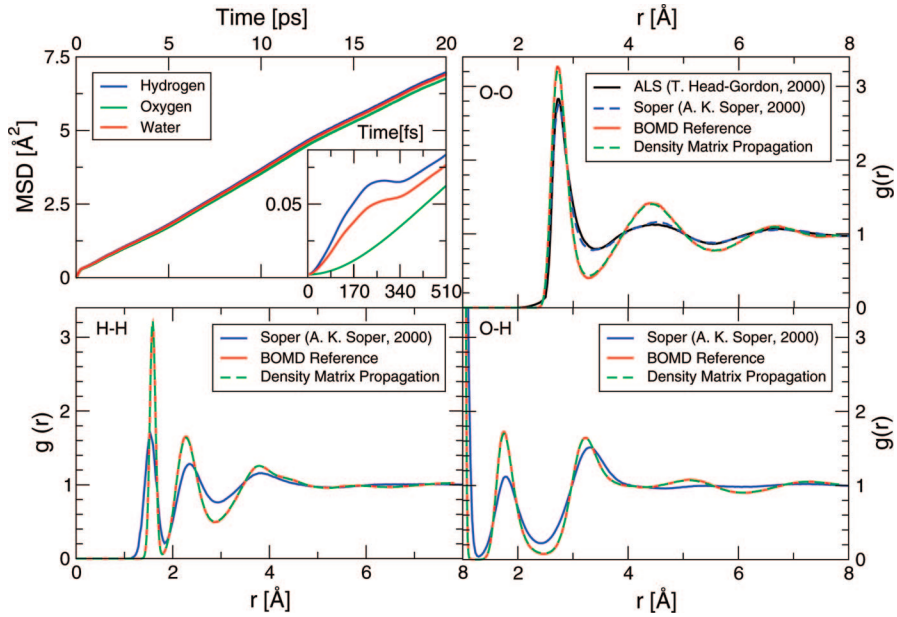

Figure 2. Partial PCF's of liquid water at ambient conditions and its mean square displacement (top left panel). From the enclosed inset the onset of a cage effect can be observed at ~250 fs followed by diffusion, which is in excellent agreement with Gallo et al.[49]

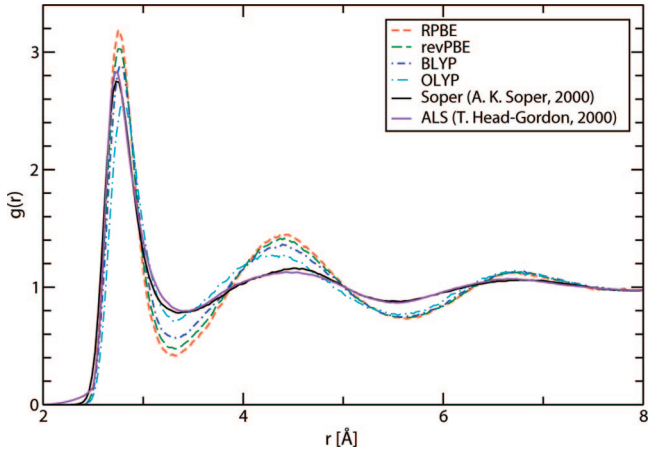

Figure 3. $g_{OO}(r)$, as obtained from neutron diffraction, X-ray scattering, and AIMD simulations using a variety of different XC functionals.

Table 1. First Maximum and Minimum Peak Heights in the $g_{OO}(r)$, Their Positions r_{OO}, and Coordination Number N_c with Respect to the XC Functional

XC	$g_{OO}^{max}(r)$	r_{OO}^{max}	$g_{OO}^{min}(r)$	r_{OO}^{min}	N_c
PBE[21]	3.25	2.73	0.44	3.28	4.04
RPBE[39]	3.19	2.75	0.42	3.32	4.03
revPBE[40]	3.01	2.77	0.50	3.31	4.05
BLYP[41,43]	2.92	2.79	0.57	3.33	4.09
OLYP[42,43]	2.57	2.79	0.71	3.30	3.90
ALS[50]	2.83	2.73	0.80	3.4	4.7
Soper[51]	2.75	2.73	0.78	3.36	–
HASY[54,55]	2.58	2.76	0.83	3.40	–
PCCP[50,55]	2.31	2.78	0.84	3.39	–

We have also performed a series of simulations using various XC functionals, as reported in Figure 3 and detailed in Table 1, that yields a coordination number ~4.0 ± 0.1 and confirms a sizable functional dependence. Nevertheless, in spite of the observed variations, and given the challenge of simulating water from first principles, all in all the performance of DFT can be judged to be encouragingly good.

The length of our simulations allows for a careful error estimation. To this end, we have randomly selected 1000 segments along the trajectory, each 25 ps long, in which we have calculated the $g_{OO}(r)$. The length of each segment is chosen to be longer than the correlation time estimated by Grossman et al.[38] The fluctuations of the $g_{OO}(r)$ in each segment relative to the average of the whole trajectory are within 2 standard deviations. This shows that given a sufficient sampling the errors in our simulations are negligible, and results from AIMD calculations are reproducible.

4.2. Hydrogen Bond Network. The textbook picture of bonding in liquid water indicates that each water molecule sits on average in a tetrahedral cage formed by a local, but macroscopically extended, HB network that is continually deformed by the dynamic breaking and re-forming of HB's. But, as already mentioned, this view has been recently challenged by Wernet et al. and is matter of current debate.[56−60] Specifically, based on X-ray absorption and Raman scattering the claim is that at ambient conditions >80% of the HB's are broken, leading to a liquid water coordination of ~2. This would imply, rather surprisingly, that liquid water predominantly consists of chains or rings.

To check whether their interpretation is coherent with our data, we use their HB definition. The corresponding results are summarized in Table 2. We find that all of our calculations support a tetrahedral arrangement, even in the case of the OLYP functional, which has the largest number of broken HB's. Since the definition of a HB is somewhat arbitrary we have also applied alternative HB definitions of Luzar and Chandler[61] as well as Kuo and Mundy.[62] The results are very similar and do not change if one slightly varies the cutoff radius or even introduces an additional persistence time criterion in the definition of HB.

Table 2. Relative Occurrence of Double Donor (DD), Single Donor (SD), No Donor (ND), Donating and Free HB's, As Obtained from AIMD Simulations Averaged over Half a Million Snapshots Using Several Semilocal XC Functionals

	PBE	RPBE	revPBE	BLYP	OLYP
DD	82.8%	81.4%	76.8%	72.9%	59.0%
SD	16.6%	17.8%	22.0%	25.4%	36.3%
ND	0.7%	0.8%	1.2%	1.7%	4.7%
donated HB's	91.0%	90.3%	87.8%	85.6%	77.1%
free HB's	9.0%	9.7%	12.2%	14.4%	22.9%
mean HB's	3.642	3.613	3.513	3.423	3.085

4.3. Dynamic Properties. Having gathered enough statistics on systems of different sizes we now address the issue of size dependence of the translational self-diffusion D. This arises from the fact that a diffusing particle sets up a hydrodynamic flow, which decays as slowly as $1/r$. In a periodically repeated system this leads to an interference between one particle and its periodic images. This effect has been analyzed by Dünweg and Kremer,[63,64] who have established the following relation for the diffusion coefficient under periodic boundary conditions as a function of simulation box length L:

$$D_{\mathrm{PBC}}(L) = D_{\infty} - \frac{k_{\mathrm{B}}T\zeta}{6\pi\eta L} \tag{3}$$

where D_{∞} is the diffusion coefficient for an infinite system, $\zeta = 2.837$ a numerical coefficient similar to the Madelung constants which results from an infinite summation over all replicas, and η the translational shear viscosity. Though this relation have been known for a while, it is not generally appreciated how large these finite size corrections might be. From Figure 4 it can be seen that, within error bars, $D_{\mathrm{PBC}}(L)$ obeys rather well the analytical $1/L$ scaling. With some caution, using eq 3, we can thus extrapolate $D_{\mathrm{PBC}}(L)$ to $L \rightarrow \infty$, in order to determine $D_{\infty} = 0.789 \times 10^{-5}$ cm^2/s, and for the first time obtain an estimate for the translational shear viscosity $\eta_{\infty} = 21.22 \times 10^{-4}$ Pa·s. These results have to be compared with the experimental values of $D = 2.395 \times 10^{-5}$ cm^2/s[65] and $\eta = 8.92 \times 10^{-4}$ Pa·s.[66] These results confirm

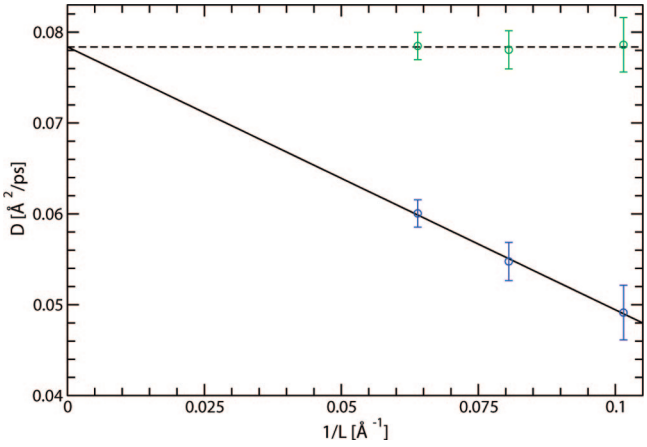

Figure 4. D_{PBC} as a function of system size, computed by AIMD simulations using the PBE XC functional. The solid line is the linear extrapolation to an infinite system, whereas the dotted line is the mean of D_{∞} corrected by eq 3.

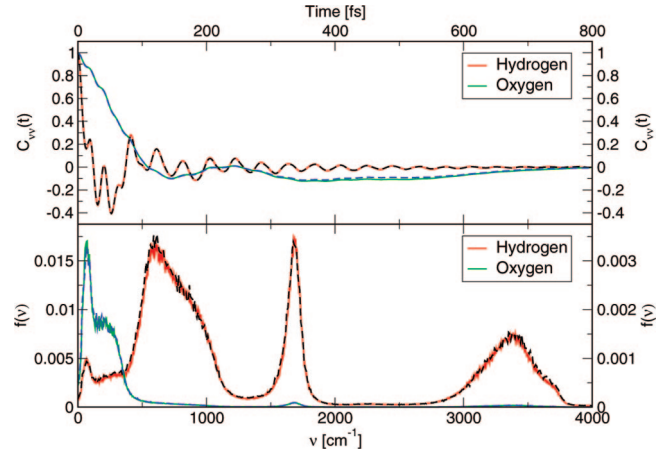

Figure 5. Velocity−velocity autocorrelation function and the power spectrum. Full lines are obtained by Car−Parrinello-like simulations, whereas dashed lines represent BOMD reference calculations.

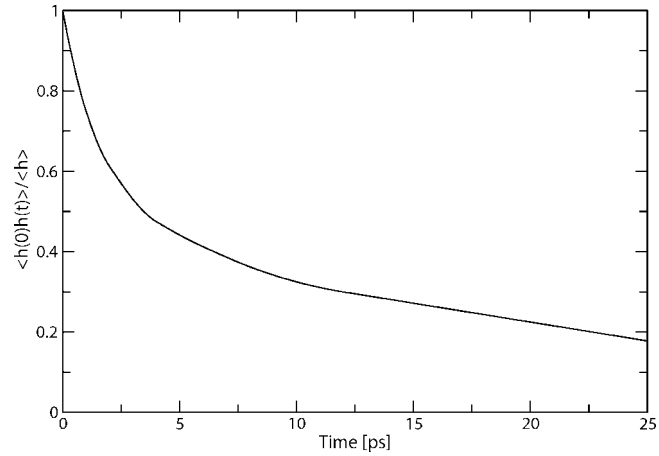

Figure 6. HB autocorrelation function as a function of simulation time.

that PBE water is less fluid than real water. However, if we take into account that we have not included nuclear quantum effects,[67,68] we conclude that PBE provides a good representation of the water potential energy surface. In addition, Figure 4 shows that for all of our simulations the value of D_{∞}, as obtained by applying eq 3 together with the now determined η_{∞}, is consistent with our initial estimate. This demonstrates that η_{∞} is much less system size dependent than D_{∞} and that the area of validity of the Stokes−Einstein relation, which indicates an inverse relation between these two quantities, is limited.

In Figure 5, we show the velocity−velocity autocorrelation function for the hydrogen and oxygen atoms, as well as its power spectrum that is the temporal Fourier transform. The latter is of particular interest, since, besides being in excellent agreement with our BOMD reference calculations, the shoulder due to dangling HB's in the oxygen−hydrogen high-frequency stretching band further indicates a mainly symmetric charge distribution and thus tetrahedral water coordination.

In all calculations $D_{\mathrm{PBC}}(L)$ is computed using Einstein's relation from the mean square displacement, and as an extra consistency check also via the Green−Kubo relation, i.e.,

by integrating the velocity−velocity autocorrelation function with respect to time.

Given the fact that our method is new and to assess the influence of the stochastic noise on the dynamics, we performed two BOMD reference calculations, one using a canonical Langevin dynamics with exactly the same damping term as before, and another one in the microcanonical NVE ensemble. The three different calculations yield results for D_{PBC} that are indistinguishable within error bars. This further strengthens our conclusion that our sampling is correct and that the use of a Langevin equation with tiny damping does not affect the dynamical properties within statistical uncertainty.

4.4. Hydrogen Bond Kinetics. The HB kinetics is studied via the Luzar−Chandler model[69] that with just two rate constants k and k' is able to describe the complex, nonexponential behavior of the following reactive flux correlation function:

$$k(t) = -\frac{\mathrm{d}c(t)}{\mathrm{d}t} = -\frac{\langle(\mathrm{d}h/\mathrm{d}t)_{t=0}[1-h(t)]\rangle}{\langle h\rangle} = kc(t) - k'n(t) \tag{4}$$

in which $c(t) = \langle h(0)h(t)\rangle/\langle h\rangle$ is the HB autocorrelation function, and $n(t) = \langle h(0)[1 - h(t)]\, H(t)\rangle/\langle h\rangle$, where $H(t)$ is unity if a selected pair of molecules are closer than the distance $R = 3.5$ Å and zero otherwise, while $\langle\bullet\rangle$ denotes temporal averages. Thus, $n(t)$ denotes the number of initially bonded pairs of molecules that are broken at time t, while remaining closer than R. In the HB population operator $h(t)$, we use the previous mentioned HB defintions. The HB lifetime is related to k by $\tau_{\mathrm{HB}} = k^{-1}$, whereas the HB relaxation time is computed as

$$\tau_{\mathrm{r}} = \frac{\int \mathrm{d}t\, tc(t)}{\int \mathrm{d}t\, c(t)} \tag{5}$$

The reactive flux correlation function $k(t)$ is nonexponential and monotonically decaying after a few libration periods. A least-squares fit of our data to eq 4 yields $k = 0.143$ ps^{-1} and $k' = 0.389$ ps^{-1}, thus $\tau_{\mathrm{HB}} = 6.98$ ps and $\tau_{\mathrm{r}} = 10.25$ ps. When compared to the classical results of Xu et al.,[70] our values for τ_{HB} and τ_{r} are both about twice as large. As a consequence, the ratio $\tau_{\mathrm{r}}/\tau_{\mathrm{HB}} = 1.47$ is very close to the value ∼1.5 reported by others.[19,70]

Besides these quantitative differences, there is also a qualitative discrepancy in the sense that in our ab initio calculation $c(t)$ decorrelates significantly slower and ceases to be exponentially decaying as displayed in Figure 6. In fact, we suspect that the decay might be biexponential, which would assume a second linear equation for $n(t)$. But in any case, this can be tentatively attributed to polarization effects that are possibly better described by DFT, though a final answer would require further investigation which is beyond the scope of this paper.

5. Conclusion

Owing to the efficiency of our novel method, to the best of our knowledge, we have presented the most extensive AIMD simulations so far. We found that structural properties are well converged and reproducible. By contrast, dynamical properties are much less established; however, recent progress in AIMD calculations[20] allowed us to calculate the shear viscosity and the HB relaxation time of liquid water for the first time from ab initio. Along the way, we also reassessed the liquid water structure that has been recently questioned, but all of our calculations further supports the well-established tetrahedral coordination of liquid water.

Acknowledgment. We thank R. Z. Khaliullin and H. Eshet for various fruitful discussions, as well as J. A. Morrone, Y. Mantz, and L. Ojamäe for useful suggestions. The generous allocation of computer time from Swiss National Supercomputing Center (CSCS) and technical support from Neil Stringfellow is kindly acknowledged.

References

(1) Rahman, A.; Stillinger, F. H. *J. Chem. Phys.* **1971**, *55*, 3336–3359.

(2) Wernet, P.; Nordlund, D.; Bergmann, U.; Cavalleri, M.; Odelius, M.; Ogasawara, H.; Näslund, L. A.; Hirsch, T. K.; Ojamäe, L.; Glatzel, P.; Petterson, L. G. M.; Nilsson, N. *Science* **2004**, *304*, 995–999.

(3) Stillinger, F. H. *Science* **1980**, *209*, 451–457.

(4) Berendsen, H. J. C.; Postma, J. P. M.; van Gunsteren, W. F.; Hermans, J. In *Intermolecular Forces*; Pullman, B. , Ed.; Reidel: Dordrecht, The Netherlands, 1981; pp 331−342.

(5) Jorgensen, W. L.; Chandrasekhar, J.; Madura, J. D.; Impey, R. W.; Klein, M. L. *J. Chem. Phys.* **1983**, *79*, 926–935.

(6) Guillot, B. *J. Mol. Liq.* **2002**, *101*, 219–260.

(7) Izvekov, S.; Parrinello, M.; Burnham, C. J.; Voth, G. A. *J. Chem. Phys.* **2004**, *120*, 10896.

(8) Jorgensen, W. L.; Tirado-Rives, J. *Proc. Natl. Acad. Sci. U.S.A.* **2005**, *102*, 6665–6670.

(9) Bukowski, R.; Szalewicz, K.; Groenenboom, G. C.; van der Avoird, A. *Science* **2007**, *315*, 1249–1252.

(10) Donchev, A. G.; Galkin, N. G.; Illarinov, A. A.; Khoruzhii, O. V.; Olevanov, M. A.; Ozrin, V. D.; Subbotin, M. V.; Tarasov, V. I. *Proc. Natl. Acad. U.S.A.* **2008**, *103*, 8613–8617.

(11) Kohn, W. *Rev. Mod. Phys.* **1999**, *71*, 1253–1266.

(12) Asthagiri, D.; Pratt, L. R.; Kress, J. D. *Phys. Rev. E* **2003**, *68*, 041505.

(13) Kuo, I.-F. W.; Mundy, C. J.; McGrath, M. J.; Siepmann, J. I.; VandeVondele, J.; Sprik, M.; Hutter, J.; Chen, B.; Klein, M. L.; Mohamed, F.; Krack, M.; Parrinello, M. *J. Phys. Chem. B* **2004**, *108*, 12990–12998.

(14) Fernández-Serra, M. V.; Artacho, E. *J. Chem. Phys.* **2004**, *121*, 11136–11144.

(15) VandeVondele, J.; Mohamed, F.; Krack, M.; Hutter, J.; Sprik, M.; Parrinello, M. *J. Chem. Phys.* **2005**, *122*, 014515.

(16) Sit, P. H.-L.; Marzari, N. *J. Chem. Phys.* **2005**, *122*, 204510.

(17) Mantz, Y. A.; Chen, B.; Martyna, G. J. *J. Phys. Chem. B* **2006**, *110*, 3540–3554.

(18) Lee, H.-S.; Tuckerman, M. E. *J. Chem. Phys.* **2006**, *125*, 154507.

(19) Lee, H.-S.; Tuckerman, M. E. *J. Chem. Phys.* **2007**, *126*, 164501.

(20) Kühne, T. D.; Krack, M.; Mohamed, F.; Parrinello, M. *Phys. Rev. Lett.* **2007**, *98*, 066401.

(21) Perdew, J. P.; Burke, K.; Ernzerhof, M. *Phys. Rev. Lett.* **1996**, *77*, 3865–3868.

(22) Caravati, S.; Bernasconi, M.; Kühne, T. D.; Krack, M.; Parrinello, M. *Appl. Phys. Lett.* **2007**, *91*, 171906.

(23) Pietrucci, F.; Caravati, S.; Bernasconi, M. *Phys. Rev. B* **2008**, *78*, 064203.

(24) Payne, M. C.; Teter, M. P.; Allan, D. C.; Arias, T. A.; Joannopoulos, J. D. *Rev. Mod. Phys.* **1992**, *64*, 1045–1097.

(25) Car, R.; Parrinello, M. *Phys. Rev. Lett.* **1985**, *55*, 2471–2474.

(26) Bornemann, F. A.; Schütte, C. *Numer. Math.* **1998**, *78*, 359–376.

(27) Pastore, G.; Smargiassi, E.; Buda, F. *Phys. Rev. A* **1991**, *44*, 6334–6347.

(28) Kolafa, J. *J. Comput. Chem.* **2004**, *25*, 335–342.

(29) Kolafa, J. *J. Chem. Phys.* **2005**, *122*, 164105.

(30) Martyna, G. J.; Tuckerman, M. E. *J. Chem. Phys.* **1995**, *102*, 8071–8077.

(31) Niklasson, A. M. N.; Tymczak, C. J.; Challacombe, M. *Phys. Rev. Lett.* **2006**, *97*, 123001.

(32) VandeVondele, J.; Hutter, J. *J. Chem. Phys.* **2003**, *118*, 4365–4369.

(33) Krajewski, F. R.; Parrinello, M. *Phys. Rev. B* **2006**, *73*, 041105(R).

(34) Berendsen, H. J. C.; Postma, J. P. M.; van Gunsteren, W. F.; DiNola, A.; Haak, J. R. *J. Chem. Phys.* **1984**, *81*, 3684–3690.

(35) Ricci, A.; Ciccotti, G. *Mol. Phys.* **2003**, *101*, 1927–1931.

(36) Goedecker, S.; Teter, M.; Hutter, J. *Phys. Rev. B* **1996**, *54*, 1703–1710.

(37) Hartwigsen, C.; Goedecker, S.; Hutter, J. *Phys. Rev. B* **1998**, *58*, 3641–3662.

(38) Krack, M. *Theor. Chem. Acc.* **2005**, *114*, 145–152.

(39) Grossman, J. C.; Schwegler, E.; Draeger, E. W.; Gygi, F.; Galli, G. *J. Chem. Phys.* **2004**, *120*, 300–311.

(40) Hammer, B.; Hansen, L. B.; Norskov, J. K. *Phys. Rev. B* **1999**, *59*, 7413–7421.

(41) Zhang, Y.; Yang, W. *Phys. Rev. Lett.* **1998**, *80*, 890–890.

(42) Becke, A. D. *Phys. Rev. A* **1988**, *38*, 3098–3100.

(43) Handy, N. C.; Cohen, A. J. *Mol. Phys.* **2001**, *99*, 403–412.

(44) Lee, C.; Yang, W.; Parr, R. G. *Phys. Rev. B* **1988**, *37*, 785–789.

(45) Lippert, G.; Hutter, J.; Parrinello, M. *Mol. Phys.* **1997**, *92*, 477–488.

(46) VandeVondele, J.; Krack, M.; Mohamed, F.; Parrinello, M.; Chassaing, T.; Hutter, J. *Comput. Phys. Commun.* **2005**, *167*, 103–128.

(47) Ceriotti, M.; Kühne, T. D.; Parrinello, M. *J. Chem. Phys.* **2008**, *129*, 024707.

(48) VandeVondele, J.; Hutter, J. *J. Chem. Phys.* **2007**, *127*, 114105.

(49) Gallo, P.; Sciortino, F.; Tartaglia, P.; Chen, S.-H. *Phys. Rev. Lett.* **1996**, *76*, 2730–2733.

(50) Hura, G.; Russo, D.; Glaeser, R. M.; Head-Gordon, T.; Krack, M.; Parrinello, M. *Phys. Chem. Chem. Phys.* **2003**, *5*, 1981–1991.

(51) Soper, A. K. *Chem. Phys.* **2000**, *258*, 121–137.

(52) Morrone, J. A.; Car, R. *Phys. Rev. Lett.* **2008**, *101*, 017801.

(53) Chen, B.; Ivanov, I.; Klein, M. L.; Parrinello, M. *Phys. Rev. Lett.* **2003**, *91*, 215503.

(54) Hart, R. T.; Benmore, C. J.; Neufeind, J.; Kohara, S.; Tomberli, B.; Egelstaff, P. A. *Phys. Rev. Lett.* **2005**, *94*, 047801.

(55) Soper, A. K. *J. Phys.: Condens. Matter* **2007**, *19*, 335206.

(56) Smith, J. D.; Cappa, C. D.; Wilson, K. R.; Messer, B. M.; Cohen, R. C.; Saykally, R. J. *Science* **2004**, *306*, 851–853.

(57) Fernández-Serra, M. V.; Artacho, E. *Phys. Rev. Lett.* **2006**, *96*, 016404.

(58) Prendergast, D.; Galli, G. *Phys. Rev. Lett.* **2006**, *96*, 215502.

(59) Head-Gordon, T.; Johnson, M. E. *Proc. Natl. Acad. Sci. U.S.A.* **2006**, *103*, 7973–7977.

(60) Iannuzzi, M. *J. Chem. Phys.* **2008**, *128*, 204506.

(61) Luzar, A.; Chandler, D. *Nature* **1996**, *379*, 55–57.

(62) Kuo, I.-F. W.; Mundy, C. J. *Science* **2004**, *303*, 658–660.

(63) Dünweg, B.; Kremer, K. *J. Chem. Phys.* **1993**, *99*, 6983–6997.

(64) Yeh, I.-C.; Hummer, G. *J. Phys. Chem. B* **2004**, *108*, 15873–15879.

(65) Hardy, E. H.; Zygar, A.; Zeidler, M. D.; Holz, M.; Sacher, F. D. *J. Chem. Phys.* **2001**, *114*, 3174–3181.

(66) Harris, K. R.; Woolf, L. A. *J. Chem. Eng. Data* **2004**, *49*, 1064–1069.

(67) Miller, T. F., III; Manolopoulos, D. E. *J. Chem. Phys.* **2005**, *123*, 154504.

(68) Paesani, F.; Zhang, W.; Case, D. A.; Cheatham, T. E., III; Voth, G. A. *J. Chem. Phys.* **2006**, *125*, 184507.

(69) Luzar, A.; Chandler, D. *Phys. Rev. Lett.* **1996**, *76*, 928–931.

(70) Xu, H.; Stern, H. A.; Berne, B. J. *J. Phys. Chem. B* **2002**, *106*, 2054–2060.

CT800417Q